

Steady and unsteady state thermal behaviour of triple concentric-tube heat exchanger

Nora Boultif¹ · Cherif Bougriou²

Received: 27 September 2015 / Accepted: 21 June 2016 / Published online: 29 June 2016
© Springer-Verlag Berlin Heidelberg 2016

Abstract This paper presents a numerical analysis by using the finite difference method to describe the steady and unsteady state thermal behavior of triple concentric-tube heat exchanger with parallel flow and counter flow arrangements. One gives the temperature variations of the three fluids and three walls with time along the triple concentric-tube heat exchanger. The fluids have a time lag and the response of triple concentric-tube heat exchanger in parallel flow configuration is faster than those of a counterflow arrangement, its performances are always lower than those of a counterflow triple concentric-tube heat exchanger. The heat transfer coefficients by convection of the three fluids vary with time in addition to the temperature and the heat exchanger performances are lower in unsteady state than the steady state case.

Abbreviations

TTHE Triple concentric tube heat exchanger
DTHE Double concentric tube heat exchanger

List of symbols

A Matrix
 B Matrix
 C_p Specific heat at constant pressure (J/kg K)
 D Diameter (m)

D_h Hydraulic diameter (m)
 G Mass velocity (kg/m²s)
 H Specific enthalpy (J/kg)
 h Heat transfer coefficient (W/m²K)
 L Length (m)
 m Mass (kg)
 \dot{m} Flowrate (kg/s)
 n Number of nodes
 Nu Nusselt number
 Pr Prandtl number
 R', R Radii (m)
 Re Reynolds number
 S Heat exchange surface (m²)
 S_c Cross section area (m²)
 Sp Pass area (m²)
 t Time (s)
 T Temperature (°C)
 V Volume (m³)
 x Coordinate
 y Coordinate

Greek letters

α Dimensionless group
 β Dimensionless group
 γ Dimensionless group
 ρ Density (kg/m³)
 λ Thermal conductivity (W/m K)
 μ Dynamic viscosity (Pa s)
 Δt Temporal discretization step (s)
 Δx Axial discretization step (m)
 Φ Heat flux (W)

Subscripts

1 Cold fluid 1
2 Cold wall 2

✉ Cherif Bougriou
cherif.bougriou@univ-batna.dz

¹ LGEM, Mechanical Engineering Department – Faculty of Technology, University of Biskra, B.P. 145, 07000 Biskra, Algeria

² LESEI, Mechanical Engineering Department – Faculty of Technology, University of Batna 2, rue, M. Boukhlouf, 05000 Batna, Algeria

3	Hot fluid 3
4	Hot wall 4
5	Cold fluid 5
6	Cold wall 6
<i>e</i>	External
<i>exp</i>	Experimental
<i>H</i>	Horizontal
<i>i</i>	Inlet, inside
<i>num</i>	Numerical
<i>o</i>	Exit
<i>V</i>	Vertical
<i>w</i>	Wall

1 Introduction

The heat exchanger is a device allowing to transfer the heat between two or more fluids through walls, without mixing them or they may be in direct contact.

The simplest model of heat exchanger that one can conceive is a simple tubular heat exchanger; it is difficult with this type of exchanger to obtain important exchange surfaces without resulting in very bulky devices. It is one of the reasons that led to develop other exchange geometries such as triple concentric-tube heat exchanger (TTHE).

The TTHE enhance the heat exchange through an additional flow passage and a high surface area is about twice that of a double concentric-tube heat exchanger (DTHE). In TTHE, we can transfer the heat between three different fluids such as: the refrigerant, the lubricant and the cooling source in a refrigeration machine.

This type of heat exchanger is frequently used in the agrifood, pharmaceutical and nuclear industries, etc. For heating, cooling, drying and pasteurization of the product, it is well suited for non-Newtonian fluids, with or without particles, for example (cheese sauce, mashed fruit, pasta, etc.).

The product to be treated generally flows in the annular space between the inner and intermediate tubes.

The literature devoted to this type of heat exchangers can be divided into two categories according to the operating conditions (steady and unsteady).

1.1 Steady state

After the first analysis conducted by Morley [1], concerning the heat transfer between three fluids in a heat exchanger, several studies: Rabinovich [2], Wolf [3] and Aldous [4] have been conducted by involving heat transfer between three fluids in parallel flow, analytical and experimental studies are then developed on (TTHE). Zuritz [5] solved the differential equations of the first order by the Laplace transform to determine the temperatures of the

three fluids in a triple concentric-tube heat exchanger in case of counterflow.

Ünal [6] developed, in the first part of his study, a mathematical model by giving the various ordinary differential equations of first and second order and solutions for both parallel flow and counterflow arrangements. In the second part [7], the results of several cases corresponding to a counter-current arrangement are presented based on analytical solutions obtained in the first part. The study of these cases includes calculations of performance and design; it showed that the relative sizes of the three tubes radii are the most important parameters that influence the effectiveness of the exchanger.

Sahoo et al. [8] developed an iterative technique based on the equations obtained from the first law of thermodynamics for the accurate estimation of heat transfer coefficients and overall heat transfer coefficients when the two surfaces are involved (the inner surface of the intermediate tube and the outer surface of the inner tube) of the triple concentric-tube heat exchanger.

Batmaz and Sandeep [9] determined the global coefficients of fluids in a (TTHE) by using the energy balance equations in a control volume. In 2008, the same authors [10], compared the effectiveness of the (TTHE) to that of a double concentric-tube heat exchanger, they observed that for counterflow assays, the values of the (TTHE) effectiveness are higher than that of the (DTHE) with the same diameters of the inner tube and outer tube. For the parallel flow, the results showed that in some cases the (DTHE) could achieve higher efficiency values than the (TTHE). The decrease in the (TTHE) efficiency is due to the crossover.

Radulescu et al. [11] have developed an algorithm for calculating the heat transfer coefficient of the fluid flowing in the inner annular space of a triple concentric-tube heat exchanger. The flow regimes in the heat exchanger are transient in the central tube and inner annular space and laminar in the outer annular space. They established a new Nusselt correlation of the annular space.

Quadir et al. [12] conducted an experimental study on performance of (TTHE) in steady state operation for two flow configurations, called N–H–C and C–H–N for insulated and uninsulated conditions. The three considered fluids are: hot water, cold water and normal tap water. Under N–H–C arrangement, normal water flows into the inner tube, the hot water flows into the inner annular space, and cold water flows into the outer annular space. All the fluids flow in parallel to one another. The cold water and the normal water are permuted in the C–H–N arrangement; the hot water flow rate remains unchanged. They concluded that the transfer of heat between the three fluids considered more effective in N–H–C configuration than the C–H–N arrangement. Quadir et al. [13] have realized a numerical

study to describe the thermal behavior of the triple concentric-tube heat exchanger with the finite element method in the steady state and for the same arrangements mentioned in their previous study [12]. They presented the results under the form of the dimensionless temperature variations of the three fluids along the heat exchanger for their different flow rates.

Pătrășcioiu and Rădulescu [14] have been developed a numerical model of predicting outlet temperatures in a triple concentric-tube heat exchanger. They have been used the equations of heat transfer and of fluid-dynamics, as well as a numerical algorithm to solve systems of non-linear equations. Nowadays, commercial CFD can and is used in analyses of this type of heat exchangers, Behera et al. [15].

1.2 Unsteady state

All the heat exchangers work in steady state. The unsteady state is the result of the fluctuations in flows supplied by pumps, the load shedding and the starting up of the thermal installations. In unsteady state, the heat conduction in walls and the heat convection in fluids of the heat exchanger depend on the time. These processes are described in detail in the work of Kakc and Yener [16]. Valladares [17] has developed a one-dimensional numerical study of the thermal performance of the triple concentric-tube heat exchangers, the governing equations are discretized by the step-by-step implicit method for fluids and a numerical scheme of implicit finite difference and the central resolution line by line to the tube walls. However, he only presented the results in steady regime, he compared them with the results obtained by Ünal [7] in order to verify and validate the numerical model.

Nema and Datta [18] present in their study a digital model that can be used to control the temperature or the pressure of the steam to overcome the milk outlet temperature drop caused by the fouling in a helical triple concentric-tube heat exchanger. The optimal operating strategy is to increase the temperature of the wall gradually to fight against heat loss due to fouling. Bielski and Malinowski [19] have solved analytically by the method of the Laplace transform, the set of partial differential equations describing the transient temperature field in a parallel flow (TTHE). The solution is obtained for a particular case of the heat exchanger with two heat connections between the two fluids, a constant temperature in a tube and an increasing temperature level at the entrance of a fluid. Nema and Datta [20] have presented in a second section an improved simulation model, which can be used to predict the thickness of the fouling and the outlet temperature of the milk in a helical triple tube heat exchanger.

In this study, we use a numerical simulation of temperature and heat transfer coefficients by convection fields of

the three fluids and three walls for both parallel flow and counterflow arrangements of single-phase heat transfer in steady and unsteady state in a triple concentric-tube heat exchanger.

The main objective of this study is to calculate numerically the time lag and the variation of heat transfer coefficients by convection of the three fluids with time in addition to the temperature along the triple concentric-tube heat exchanger in parallel flow and counterflow arrangements.

2 Mathematical formulation

2.1 Description of the heat exchanger

The proposed heat exchanger for this study consists of three coaxial tubes. The first fluid “1” passes through the central tube of internal and external radii inside R_2 and R'_2 respectively, the second fluid “3” enters in the internal annular space of internal and external radii R_4 and R'_4 respectively, and the third fluid “5” passes through the external annulus of internal and external radii R_6 and R'_6 respectively.

The three fluids can circulate in the same direction (parallel flow) or in the opposite direction (counterflow). These three fluids are separated by metal walls “2” and “4” through, which the heat exchanges take place by heat conduction. The heat transfer between the fluids and the walls is realised by heat convection. The outer tube wall “6” is used to separate the fluid “5” from the external environment as shown in Fig. 1.

This study was conducted under the following assumptions:

- Unsteady operating regime.
- Constant flow sections.
- Completely insulated heat exchanger.
- Monophasic and incompressible fluids.
- Thermophysical properties of the fluids vary with temperature.
- Axial heat conduction only in the walls.
- One-dimensional calculus.
- Turbulent flow regimes.

Our study is based on the energy balances performed on each fluid and on each wall. The heat exchanger is divided in length volumes Δx in each of these volumes, the properties of the fluid and the solid are assumed constant at any given time, Fig. 2:

$$\Phi_{H|X-\Delta X/2} - \Phi_{H|X+\Delta X/2} + \Phi_{V|y} - \Phi_{V|y+\Delta y} = mC_p \frac{\partial T}{\partial t} \quad (1)$$

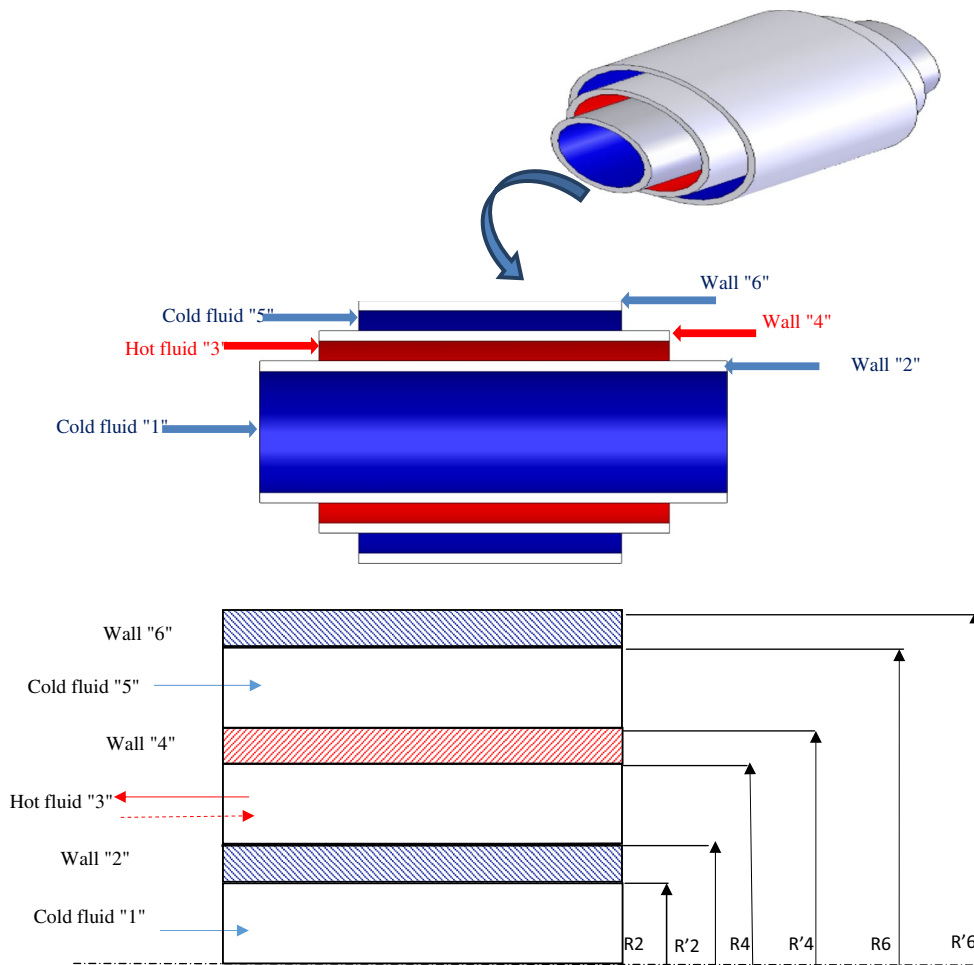


Fig. 1 Longitudinal section of the triple concentric tube heat exchanger

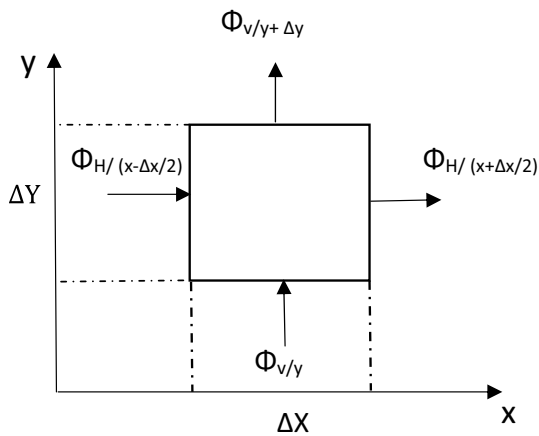


Fig. 2 Global energy balance

Counterflow case

In the case of a methodical flow, one replaces the heat flux through their next expressions:

$$\Phi_H = -\lambda S_c \frac{\partial T}{\partial X} \quad \text{for walls} \tag{2}$$

$$\Phi_H = \dot{m}H \quad \text{for fluids} \tag{3}$$

$$\Phi_v = h S \frac{\partial T}{\partial X} \tag{4}$$

The heat balance for each wall and fluid is given by the following expressions:

Wall "6"

$$-\lambda S_{c6} \frac{\partial T}{\partial X} \Big|_{X-\Delta X/2} + \lambda S_{c6} \frac{\partial T}{\partial X} \Big|_{X+\Delta X/2} + h_5 S_5 \Delta T_5 = (mC_p)_6 \frac{\partial T}{\partial t} \tag{5}$$

Fluid "5"

$$\dot{m}H|_{X-\Delta X/2} - \dot{m}H|_{X+\Delta X/2} + h_5 S_4 \Delta T_4 - h_5 S_5 \Delta T_5 = (mC_p)_5 \frac{\partial T}{\partial t} \tag{6}$$

Wall “4”

$$-\lambda S_{c4} \frac{\partial T}{\partial X} \Big|_{X-\Delta X/2} + \lambda S_{c4} \frac{\partial T}{\partial X} \Big|_{X+\Delta X/2} + h_3 S_3 \Delta T_3 - h_5 S_4 \Delta T_4 = (mC_P)_4 \frac{\partial T}{\partial t} \quad (7)$$

Fluid “3”

$$-\dot{m}H|_{X-\Delta X/2} + \dot{m}H|_{X+\Delta X/2} - h_3 S_3 \Delta T_3 - h_3 S_2 \Delta T_2 = (mC_P)_3 \frac{\partial T}{\partial t} \quad (8)$$

Wall “2”

$$-\lambda S_{c2} \frac{\partial T}{\partial X} \Big|_{X-\Delta X/2} + \lambda S_{c2} \frac{\partial T}{\partial X} \Big|_{X+\Delta X/2} + h_3 S_2 \Delta T_2 - h_1 S_1 \Delta T_1 = (mC_P)_2 \frac{\partial T}{\partial t} \quad (9)$$

Fluid “1”

$$\dot{m}H|_{X-\Delta X/2} - \dot{m}H|_{X+\Delta X/2} + h_1 S_1 \Delta T_1 = (mC_P)_1 \frac{\partial T}{\partial t} \quad (10)$$

The initial condition at any point on the heat exchanger is such that at $t = 0$.

$$T(X, 0) = T_0 \quad (11)$$

The boundary conditions for each fluid and wall are given by:

Walls “2”, “4” and “6”

$$\frac{\partial T}{\partial X}(L, t) = \frac{\partial T}{\partial X}(0, t) = 0 \quad (12)$$

Fluid “3”

$$T_3(L, t) = T_{\text{imposed}} \quad (13)$$

Fluids “5” and “1”

$$T_5(0, t) = T_1(0, t) = T_{\text{imposed}} \quad (14)$$

Parallel flow case

In the case of parallel flow heat exchanger, the energy balance can be written in the same manner as above; the only equation that has a new form is that of the hot fluid (3):

Fluid “3”

$$\dot{m}H|_{X-\Delta X/2} - \dot{m}H|_{X+\Delta X/2} - h_3 S_3 \Delta T_3 - h_3 S_2 \Delta T_2 = (mC_P)_3 \frac{\partial T}{\partial t} \quad (15)$$

with boundary condition

$$T_3(0, t) = T_{\text{imposed}} \quad (16)$$

3 Numerical resolution

An implicit finite differences scheme was used for the discretization of the above equations, as an example, one gives the discretization of the equations of the wall “6” and fluid “3”:

Wall “6”

The Eq. (5) of the wall “6” is transformed by substituting the partial derivatives by the finite differences:

$$\lambda_6 S_{C6} \frac{(T_{X-\Delta X} - T_X)}{\Delta X^2} - \lambda_6 S_{C6} \frac{(T_X - T_{X+\Delta X})}{\Delta X^2} + h_5 S_5 \Delta T_5 = (mcp)_6 \frac{T^{new} - T^{old}}{\Delta t} \quad (17)$$

We have:

$$V_6 = S_{C6} \Delta X = \pi (R_6^2 - R_6'^2) \Delta X \quad (18)$$

$$S_5 = 2\pi (R_6) \Delta X \quad (19)$$

Dividing the Eq. (17) by V_6 and multiplying by $\frac{\Delta t}{(\rho cp)_6}$, we find:

$$\frac{\Delta t}{(\rho cp)_6} \frac{\lambda_6}{\Delta X^2} (T_{X-\Delta X} - 2T_X + T_{X+\Delta X}) + h_5 \frac{\Delta t}{(\rho cp)_6} \left(\frac{2R_6}{R_6'^2 - R_6^2} \right) (T_5 - T_X) = T^{new} - T^{old} \quad (20)$$

With this arrangement some dimensionless groups appear:

$$\alpha_6 = \frac{\Delta t}{(\rho cp)_6} \frac{\lambda_6}{\Delta X^2} \quad (21)$$

$$\beta_6 = h_5 \frac{\Delta t}{(\rho cp)_6} \left(\frac{2R_6}{R_6'^2 - R_6^2} \right) \quad (22)$$

The final writing of the equation becomes:

$$\alpha_6 (T_{X-\Delta X} - 2T_X + T_{X+\Delta X}) + \beta_6 (T_5 - T_X) = T^{new} - T^{old} \quad (23)$$

Fluid 3

Knowing that

$$H = cp\Delta t \quad (24)$$

$$\dot{m} = GS_P \quad (25)$$

Enthalpies were replaced by the temperature by using a decentered scheme of the finite differences method (upwind scheme), Spalding [21].

The Eq. (8) of fluid “3” becomes:

$$Sp_3(Gcp)_3(T_{X+\Delta X} - T_X) - h_3S_3(T_X - T_4) - h_3S_2(T_X - T_2) = (mcp)_3 \frac{T^{new} - T^{old}}{\Delta t} \quad (26)$$

with

$$V_3 = Sp_3\Delta X = \pi(R_4^2 - R_2^2)\Delta X \quad (27)$$

$$S_3 = 2\pi R_4\Delta X \quad (28)$$

$$S_2 = 2\pi R_2'\Delta X \quad (29)$$

Dividing the Eq. (26) by V_3 and multiplying by $\frac{\Delta t}{(\rho cp)_3}$, we find:

$$\frac{G_3\Delta t}{\rho\Delta X}(T_{X+\Delta X} - T_X) - \frac{h_3\Delta t}{(\rho cp)_3} \left(\frac{2R_2'}{R_4^2 - R_2^2} \right) (T_X - T_4) - \frac{h_3\Delta t}{(\rho cp)_3} \left(\frac{2R_4}{R_4^2 - R_2^2} \right) (T_X - T_2) = T^{new} - T^{old} \quad (30)$$

by putting:

$$\alpha_3 = \frac{G_3\Delta t}{\rho\Delta X} \quad (31)$$

$$\beta_3 = \frac{h_3\Delta t}{(\rho cp)_3} \left(\frac{2R_2'}{R_4^2 - R_2^2} \right) \quad (32)$$

$$\gamma_3 = \frac{h_3\Delta t}{(\rho cp)_3} \left(\frac{2R_4}{R_4^2 - R_2^2} \right) \quad (33)$$

The final equation takes the following form:

$$\alpha_3(T_{X+\Delta X} - T_X) - \beta_3(T_X - T_4) - \gamma_3(T_X - T_2) = T^{new} - T^{old} \quad (34)$$

The other equations are discretized in the same manner, the dimensionless groups are assumed constant at any given time, and they represent the variation of the thermophysical properties of fluids and solids along the heat exchanger. By decreasing the elements of volume, the made supposition by considering that the thermophysical properties vary with the temperature gets closer of the reality.

The systems of equations are established, the new temperature T^{new} where $T^{(k+1)}$ is explicitly defined in terms of old temperatures T^{old} where T^k . It is easy to program and use the explicit formula, by requiring very strict stability criteria.

The implicit technique is stable, but if the time step Δt is too large, the truncation errors occur, these errors also cause oscillations in the results. The best solution can be adapted by the scheme of Crank–Nicholson, Nougier [22].

Equations (23) and (34) become:

Wall “6”

$$\frac{\alpha_{6,j}}{2} (T_{6,j-1}^{k+1} + T_{6,j-1}^k) - \frac{\alpha_{6,j}}{2} (2T_{6,j}^{k+1} + 2T_{6,j}^k) + \frac{\alpha_{6,j}}{2} (T_{6,j+1}^{k+1} + T_{6,j+1}^k) + \beta_{6,j}T_{5,j}^k - \frac{\beta_{6,j}}{2} (T_{6,j}^{k+1} + T_{6,j}^k) = T_{6,j}^{k+1} - T_{6,j}^k \quad (35)$$

After arranging the terms, Eq. (35) is written in the form:

$$\frac{\alpha_{6,j}}{2}T_{6,j-1}^{k+1} - \left(\alpha_{6,j} + \frac{\beta_{6,j}}{2} + 1 \right) T_{6,j}^{k+1} + \frac{\alpha_{6,j}}{2}T_{6,j+1}^{k+1} = B_{6(j)} \quad (36)$$

with

$$B_{6(j)} = -\frac{\alpha_{6,j}}{2}T_{6,j-1}^k + \left(\alpha_{6,j} + \frac{\beta_{6,j}}{2} - 1 \right) T_{6,j}^k - \beta_{6,j}T_{5,j}^k \quad (37)$$

The matrix writing of the previous equations is given by:

- For $j = 1$

$$A(1, 1) = -\left(\frac{\alpha_{6,1}}{2} + \frac{\beta_{6,1}}{2} + 1 \right)$$

$$A(1, 2) = \frac{\alpha_{6,1}}{2}$$

$$B_{6(1)} = +\left(\alpha_{6,1} + \frac{\beta_{6,1}}{2} - 1 \right) T_{6,1}^k - \frac{\alpha_{6,1}}{2}T_{6,2}^k - \beta_{6,1}T_{5,1}^k$$

- For $j = 2, N-1$

$$A(j, j-1) = \frac{\alpha_{6,j}}{2}$$

$$A(j, j) = -\left(\alpha_{6,j} + \frac{\beta_{6,j}}{2} + 1 \right)$$

$$A(j, j+1) = \frac{\alpha_{6,j}}{2}$$

$$B_{6(j)} = -\frac{\alpha_{6,j}}{2} T_{6,j-1}^k + \left(\alpha_{6,j} + \frac{\beta_{6,j}}{2} - 1 \right) T_{6,j}^k - \frac{\alpha_{6,j}}{2} T_{6,j+1}^k - \beta_{6,j} T_{5,j}^k$$

- For $j = N$

$$A(N, N - 1) = \frac{\alpha_{6,N}}{2}$$

$$A(N, N) = -\left(\frac{\alpha_{6,N}}{2} + \frac{\beta_{6,N}}{2} + 1 \right)$$

$$B_{6(N)} = \frac{\alpha_{6,N}}{2} T_{6,N-1}^k + \left(\frac{\alpha_{6,N}}{2} + \frac{\beta_{6,N}}{2} - 1 \right) T_{6,N}^k - \beta_{6,N} T_{5,N}^k$$

The final matrix form is:

$$\begin{bmatrix} A(1, 1) & A(1, 2) & 0 & 0 & 0 & 0 & 0 & 0 & 0 & 0 & 0 \\ A(2, 1) & A(2, 2) & A(2, 3) & 0 & \cdot & \cdot & \cdot & \cdot & \cdot & \cdot & \cdot \\ 0 & \cdot & \cdot & \cdot & 0 & \cdot & \cdot & \cdot & \cdot & \cdot & \cdot \\ 0 & 0 & \cdot & \cdot & \cdot & 0 & \cdot & \cdot & \cdot & \cdot & \cdot \\ 0 & \cdot & 0 & A(j, j - 1) & A(j, j) & A(j, j + 1) & 0 & \cdot & \cdot & \cdot & \cdot \\ 0 & \cdot & \cdot & 0 & \cdot & \cdot & \cdot & 0 & \cdot & \cdot & \cdot \\ 0 & \cdot & \cdot & \cdot & 0 & \cdot & \cdot & \cdot & \cdot & \cdot & \cdot \\ 0 & \cdot & \cdot & \cdot & \cdot & 0 & \cdot & \cdot & \cdot & \cdot & \cdot \\ 0 & \cdot & \cdot & \cdot & \cdot & \cdot & 0 & \cdot & \cdot & A(N - 1, N) & \cdot \\ 0 & 0 & 0 & 0 & 0 & 0 & 0 & 0 & A(N, N - 1) & A(N, N) & \cdot \end{bmatrix} \times \begin{bmatrix} T_6(1) \\ T_6(2) \\ \cdot \\ \cdot \\ T_6(j) \\ \cdot \\ \cdot \\ \cdot \\ T_6(N - 1) \\ T_6(N) \end{bmatrix} = \begin{bmatrix} B_6(1) \\ B_6(2) \\ \cdot \\ \cdot \\ B_6(j) \\ \cdot \\ \cdot \\ \cdot \\ B_6(N - 1) \\ B_6(N) \end{bmatrix}$$

with

$$B_3(j) = -\frac{\alpha_{3,j}}{2} T_{3,j+1}^k + \left(\frac{\alpha_{3,j}}{2} + \frac{\beta_{3,j}}{2} + \frac{\gamma_{3,j}}{2} - 1 \right) T_{3,j}^k - \beta_{3,j} T_{2,j}^k - \gamma_{3,j} T_{4,j}^k \tag{40}$$

The matrix writing of the previous equation is:

- For $j = 1, N - 1$

$$A(j, j) = -\left(\frac{\alpha_{3,j}}{2} + \frac{\beta_{3,j}}{2} + \frac{\gamma_{3,j}}{2} + 1 \right)$$

$$A(j, j + 1) = \frac{\alpha_{3,j}}{2}$$

Fluid 3

$$\frac{\alpha_{3,j}}{2} (T_{3,j+1}^{k+1} + T_{3,j+1}^k) - \frac{\alpha_{3,j}}{2} (T_{3,j}^{k+1} + T_{3,j}^k) - \frac{\beta_{3,j}}{2} (T_{3,j}^{k+1} + T_{3,j}^k) + \beta_{3,j} T_{2,j}^k - \frac{\gamma_{3,j}}{2} (T_{3,j}^{k+1} + T_{3,j}^k) + \gamma_{3,j} T_{4,j}^k = T_{3,j}^{k+1} - T_{3,j}^k \tag{38}$$

After arranging, the above equation takes the following final form:

$$\frac{\alpha_{3,j}}{2} T_{3,j+1}^{k+1} - \left(\frac{\alpha_{3,j}}{2} + \frac{\beta_{3,j}}{2} + \frac{\gamma_{3,j}}{2} + 1 \right) T_{3,j}^{k+1} = BL_3(j) \tag{39}$$

$$B_3(j) = -\frac{\alpha_{3,j}}{2} T_{3,j+1}^k + \left(\frac{\alpha_{3,j}}{2} + \frac{\beta_{3,j}}{2} + \frac{\gamma_{3,j}}{2} - 1 \right) T_{3,j}^k - \beta_{3,j} T_{2,j}^k - \gamma_{3,j} T_{4,j}^k$$

- For $j = N$ “imposed temperature”

The matrix form is:

$$\begin{bmatrix} A(1, 1) & A(1, 2) & 0 & 0 & 0 & 0 & 0 & 0 & 0 & 0 & 0 \\ 0 & A(2, 2) & A(2, 3) & 0 & \cdot & \cdot & \cdot & \cdot & \cdot & \cdot & \cdot \\ 0 & 0 & \cdot & \cdot & 0 & \cdot & \cdot & \cdot & \cdot & \cdot & \cdot \\ 0 & 0 & 0 & \cdot & \cdot & 0 & \cdot & \cdot & \cdot & \cdot & \cdot \\ 0 & \cdot & 0 & A(j, j - 1) & A(j, j) & 0 & 0 & \cdot & \cdot & \cdot & \cdot \\ 0 & \cdot & \cdot & 0 & \cdot & \cdot & 0 & 0 & \cdot & \cdot & \cdot \\ 0 & \cdot & \cdot & \cdot & 0 & \cdot & \cdot & 0 & 0 & \cdot & \cdot \\ 0 & \cdot & \cdot & \cdot & \cdot & 0 & \cdot & \cdot & 0 & \cdot & \cdot \\ 0 & \cdot & \cdot & \cdot & \cdot & \cdot & 0 & \cdot & \cdot & \cdot & \cdot \\ 0 & 0 & 0 & 0 & 0 & 0 & 0 & 0 & A(N - 1, N - 1) & A(N - 1, N) & \cdot \end{bmatrix} \times \begin{bmatrix} T_3(1) \\ T_3(2) \\ \cdot \\ \cdot \\ T_3(j) \\ \cdot \\ \cdot \\ \cdot \\ T_3(N - 1) \end{bmatrix} = \begin{bmatrix} B_3(1) \\ B_3(2) \\ \cdot \\ \cdot \\ B_3(j) \\ \cdot \\ \cdot \\ \cdot \\ B_3(N - 1) \end{bmatrix}$$

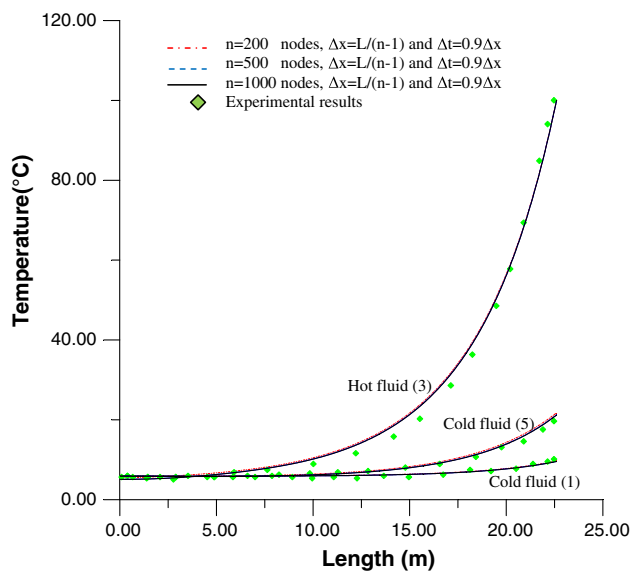


Fig. 3 Validation of the present code with the experimental results [10]

Once the equations, boundary conditions and initial conditions are discretized, the systems of equations are put under the form of the dominant diagonal matrices.

3.1 Implementation

From the input data, the computer program (Triple-Trans) distributes nodal positions in the entire heat exchanger. An initial temperature is then assigned to all nodes for the time $t = 0$. The subroutines are called to compute thermophysical properties of fluids and the calculation of local heat transfer coefficients from the Nusselt correlations for flow in a tube and in annulus, Sieder and Tate [23].

$$Nu = 0.027Re^{0.8}Pr^{0.33} \left(\frac{\mu}{\mu_w} \right)^{0.14} \quad (41)$$

Table 1 Dimensions and the thermophysical properties of fluids of the triple concentric-tube heat exchanger [10]

Dimensions and properties	Central tube	Intermediate tube	External tube
R_i (m)	0.0238	0.0301	0.0365
R_e (m)	0.0254	0.0318	0.0381
L (m)	22.6	22.6	22.6
Fluid	Propylene glycol	Water	Propylene glycol
C_p (kJ/kg K)	3.956	4.175	3.978
ρ (kg/m ³)	1025	989	1025
Volumetric flow rate (gal/min)	40.5	13.4	4.0
T_i (°C)	5.9	100.0	5.9
T_o (°C)	10.7	6.1	19.9

$$Nu = \frac{hD_h}{\lambda}$$

After that, the dimensionless groups used in the heat equations are calculated and the subroutine containing the iterative Gauss–Seidel is called to solve the heat equation for each node and provides a new temperature distribution for a step of time Δt the resolution of the temperature distribution takes place simultaneously. New temperatures are compared to previous ones, if the difference is greater than 0.01 (convergence criterion) the program will calculate the distributions for another time step, otherwise the calculations of temperature distributions are stopped and the steady state is reached.

4 Results and discussions

After establishing the mathematical model and the method of solution, the computations were executed on several grids and time steps. As illustrated in Fig. 3, a close accord is observed between several tested computational meshes. The mesh corresponding to 200 nodes (199 cells) was therefore adopted for all numerical simulations, in order to optimize the calculating time and with ample precision.

4.1 Validation

To give more confidence to the results of our numerical simulation, our code was validated with the numerical results of Batmaz and Sandeep [10]. Thermophysical properties of hot and cold fluids and heat exchanger dimensions are given in Table 1 and [10]. The thermophysical properties given by Batmaz and Sandeep are independent of the temperature

As shown in Fig. 3, it is clear that our results concerning the axial distribution of the three fluid temperatures (“1”, “3” and “5”) of counterflow triple concentric-tube heat exchanger in steady state are in good agreement with the experimental results of Batmaz and Sandeep [10].

Fig. 4 Profiles of three fluid temperatures in unsteady regime (counterflow arrangement)

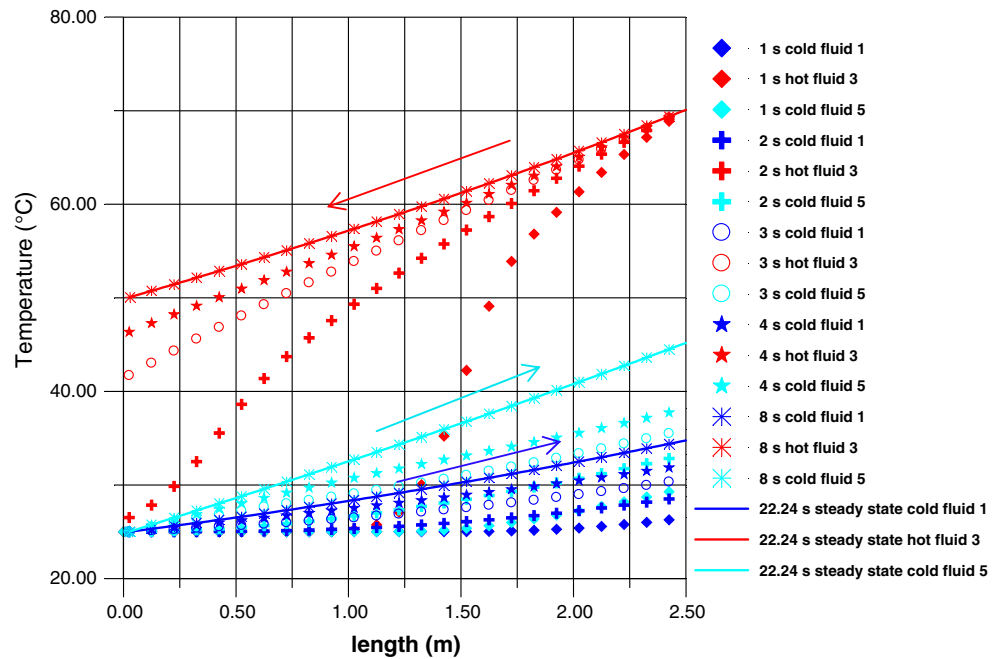
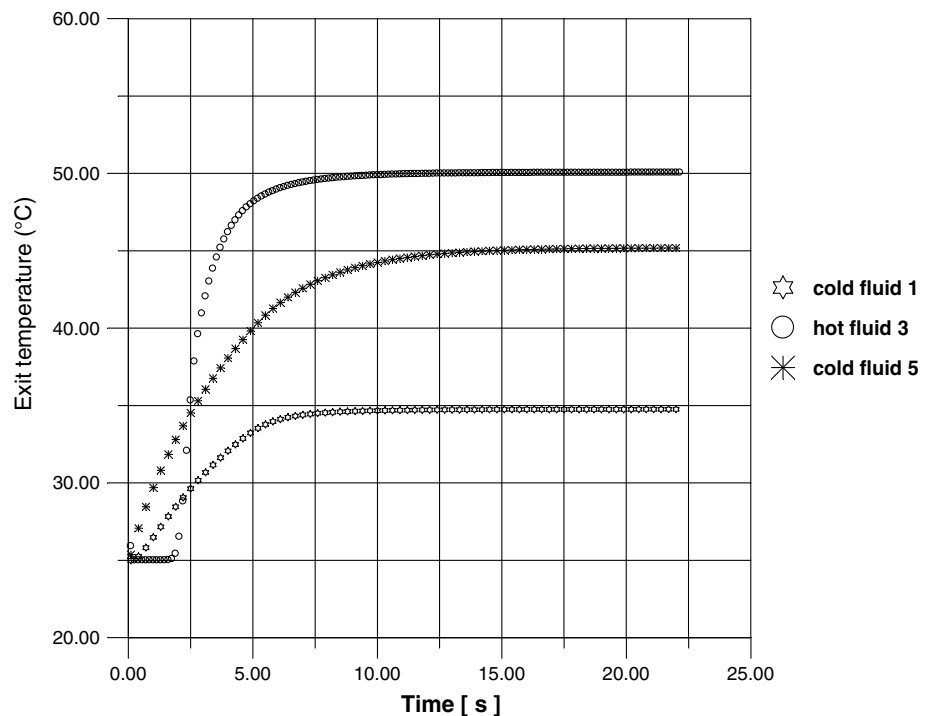


Fig. 5 Variation of three fluid outlet temperatures with the time



For fluids “1” and “5”, a perfect match is observed between the experimental and numerical results, the relative error calculated by the formula $\left| \frac{T_{exp} - T_{num}}{T_{exp}} \right|$ does not exceed 4 %, and the curves are nearly coincident.

For the hot fluid “3”, the maximum relative error between the numerical and experimental results is about 9 %. A very good consistency of results is observed.

4.2 Discussions

Our numerical model is validated in steady state due to the lack of the numerical or experimental results concerning this type of heat exchanger in unsteady regime, so in what follows, we present the behavior of this heat exchanger in unsteady regime.

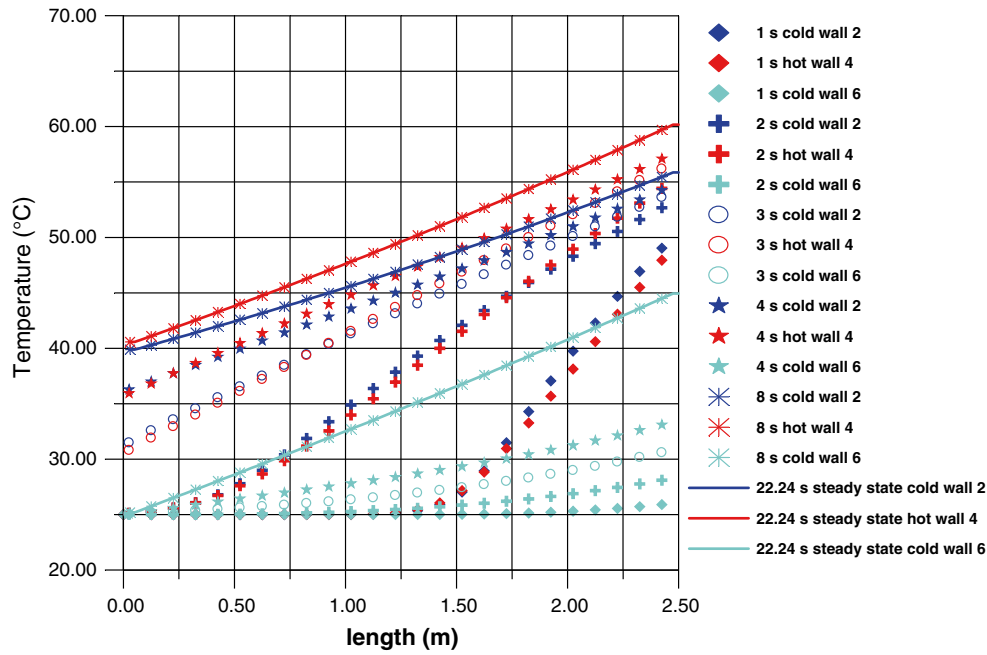
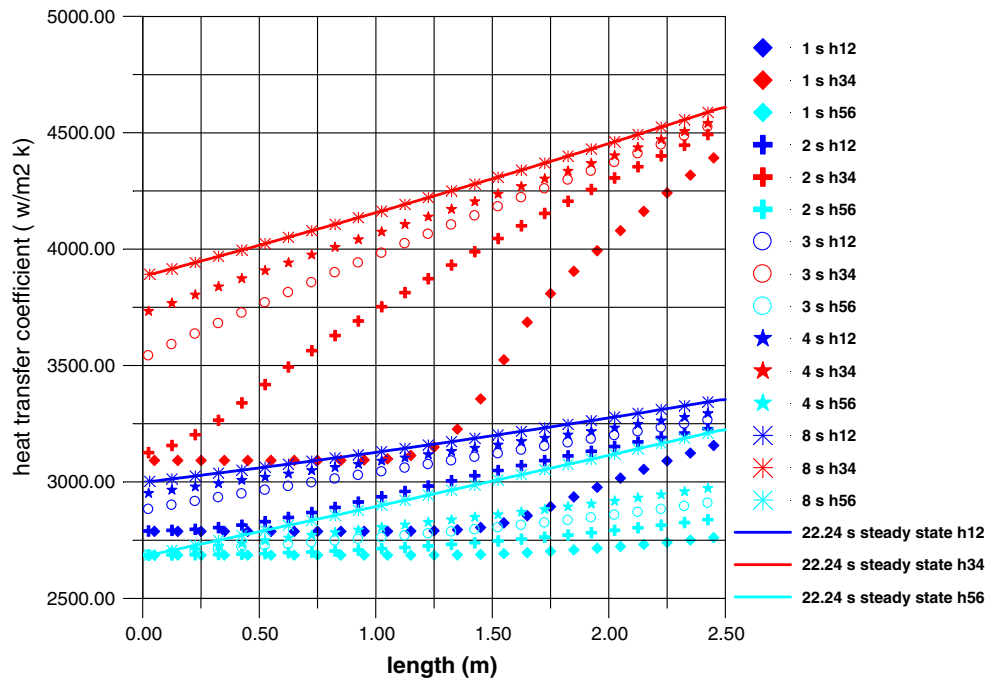


Fig. 6 Profiles of the temperatures of three walls with the time (counterflow)

Fig. 7 Variation of heat exchange coefficients by convection of the three fluids with time



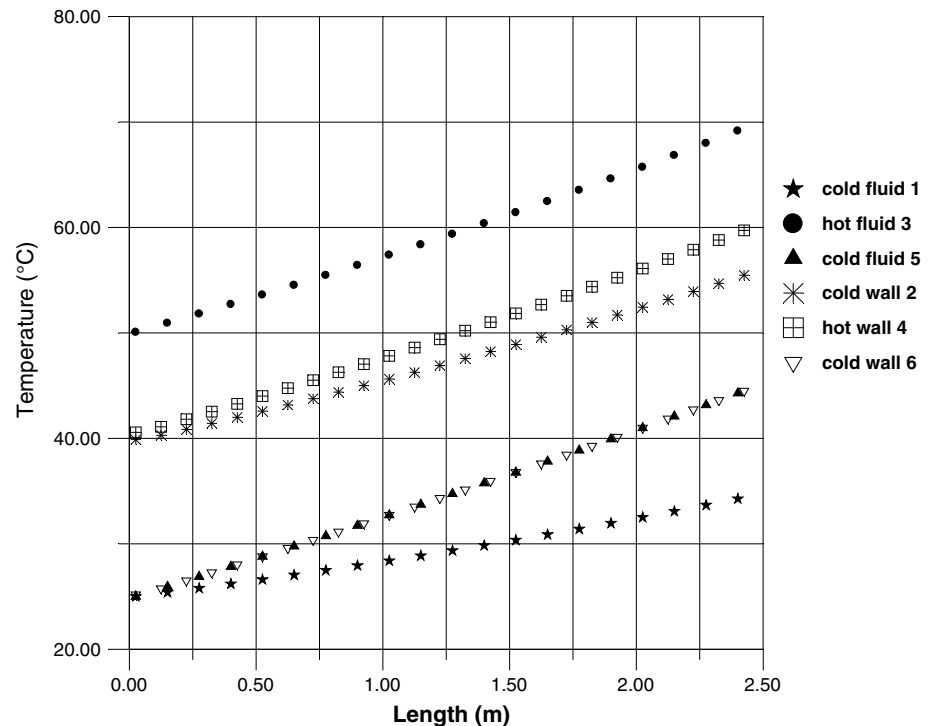
4.2.1 Counterflow arrangement

Fields temperatures inside the counterflow triple concentric-tube heat exchanger in unsteady regime are given in Fig. 4. We note that the time required for passage of the unsteady regime to steady state is 22.24 s, in the first second, the heat transfer is performed only for the half of the

heat exchange surface from the inlet of hot fluid 3. The rate of the heat exchange surface which, participates in heat transfer reaches, 100 % after 2 s. This time represents the time lag proved experimentally by El-Wakil et al. [24] and Guellal et al. [25].

As shown in Fig. 5, one gives the variation of the outlet temperatures of the three fluids flowing in counterflow

Fig. 8 Variation of temperatures of the three fluids and three walls in steady state (counterflow)



arrangement, it is clear that the hot fluid “3” has a time lag of about 2 s. After this time interval, the outlet temperature increases until the establishment of the steady state. The cold fluids “1” and “5” have no time lag.

Figure 6 shows the variation with time of the temperatures of the three walls of the heat exchanger. At time $t = 0$, the three walls were at a temperature of 25 °C. In the case of the counterflow arrangement, the cold walls “2” and “6” warms faster by going towards the heat exchanger exit and this is due to the entry of the hot fluid. The temperature of the cold wall “2” is very close to that of the hot wall because the coefficient of heat transfer of the cold fluid flowing in the tube “1” is higher than that of the fluid “5”, see Fig. 7. The steady state for the walls is reached during the same time as that of fluids.

We note in unsteady state, that the three heat exchange coefficients by convection of three fluids increase over time; this proves that the thermophysical properties of fluids depend on temperature and time. As shown in Fig. 7, the heat exchange is more efficient in steady state.

The evolution of the three-fluid temperatures and the three walls in the steady state are given in Fig. 8, the temperature of each intermediate wall is between the fluid temperatures in contact. The temperature of the wall “6” is equal to the fluid “5” because it is assumed adiabatic. The fluid “5” heat up faster because of its large heat exchange surface.

4.2.2 Parallel flow

Figure 9 shows the evolution of temperatures of the three fluids in the triple concentric tube heat exchanger at unsteady state in parallel flow arrangement. Note that the heat transfer for the three fluids is faster than in the case of a counterflow heat exchanger. This is due to the entry of fluids by the same side (the fluids are in direct thermal contact at the entrance of the device). In the first second, the hot fluid side “3” is involved in heat exchange for 1.5 m of the heat exchanger length and 1.25 m of the heat exchanger length corresponding to the cold fluids “1” and “5” participates in the exchange of heat, the steady state is established after 16.30 s.

Unlike the counterflow arrangement, the three fluids have a time lag, it is the same for both cold fluids and it is the same for the hot fluid for the two arrangements as it illustrated in Figs. 9 and 10 which, show the temporal evolution of the three fluids outlet temperatures. The cooling of the hot fluid and the heating of the cold fluids are less important than in the case of a counterflow arrangement. The temperatures of the walls “2” and “4” have the same profile as that of the hot fluid temperature “3”. The temperature of the wall “4” is higher than the temperature of the other walls because the heat exchanges are more intense (the exchange surface is larger). The wall “6” is adiabatic and follows the profile of the cold fluid “5”, see Figs. 11, 12 and 13.

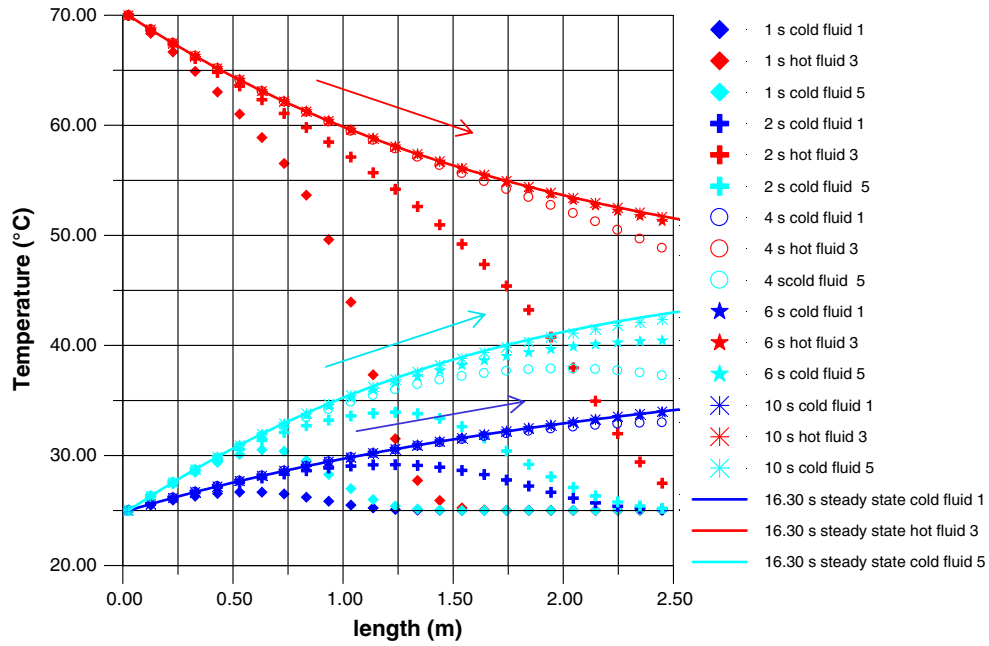
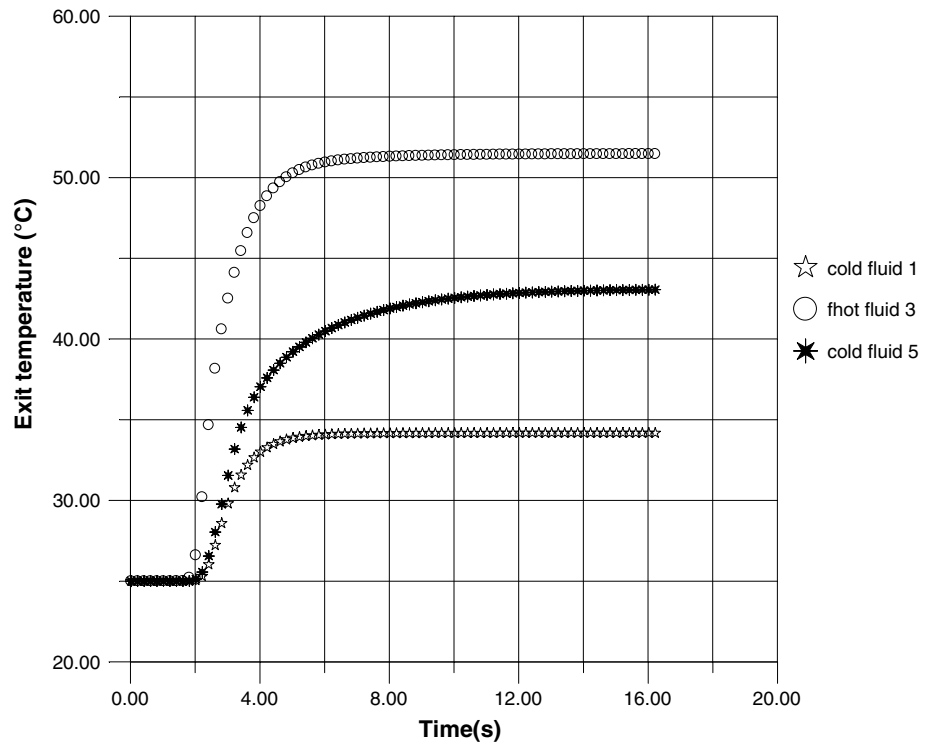


Fig. 9 Profiles of the temperatures of three fluids of the heat exchanger in unsteady state (parallel flow arrangement)

Fig. 10 Variation of the outlet temperatures of three fluids with the time (parallel flow arrangement)



The performance or the heat exchanger efficiency in unsteady state is lower than the steady state case because the temperature rise of the cold fluids and the temperature

reduction of the hot fluid are higher in the steady state (Figs. 4 and 9). In the initial condition the hot fluid temperature is supposed equal to the cold fluid temperature.

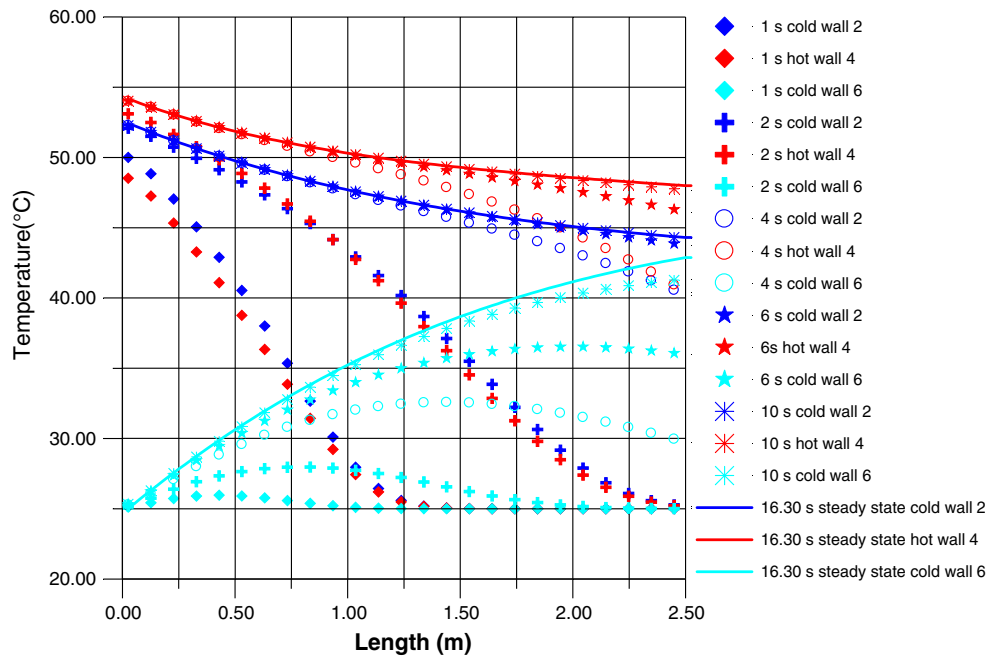
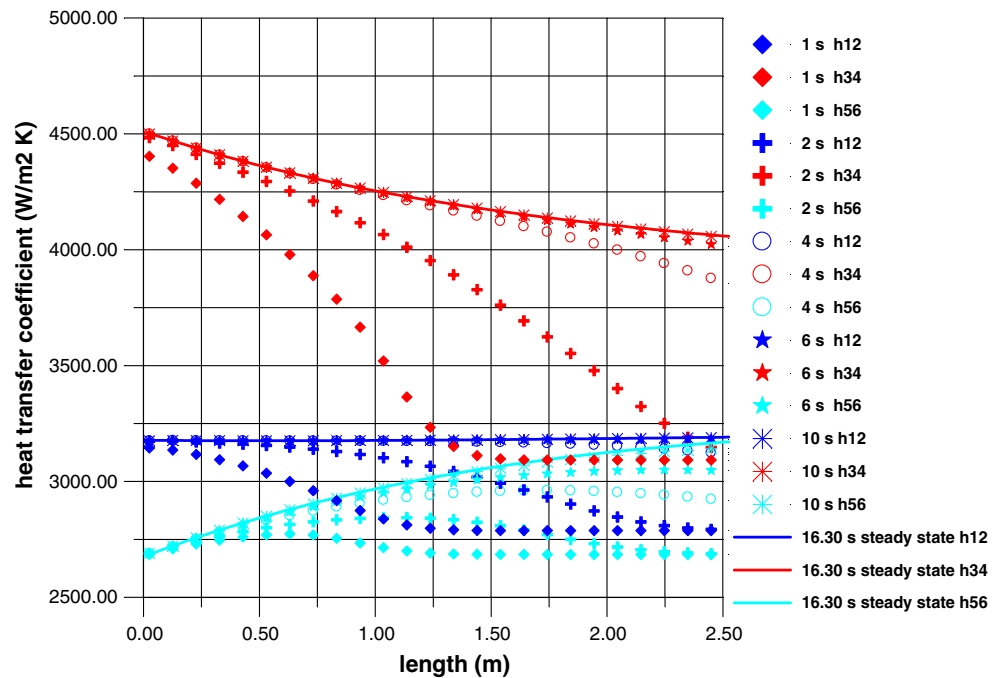


Fig. 11 Wall temperature profiles in unsteady state (parallel flow arrangement)

Fig. 12 Heat exchange coefficients profiles of the three fluids vs. time (parallel flow arrangement)



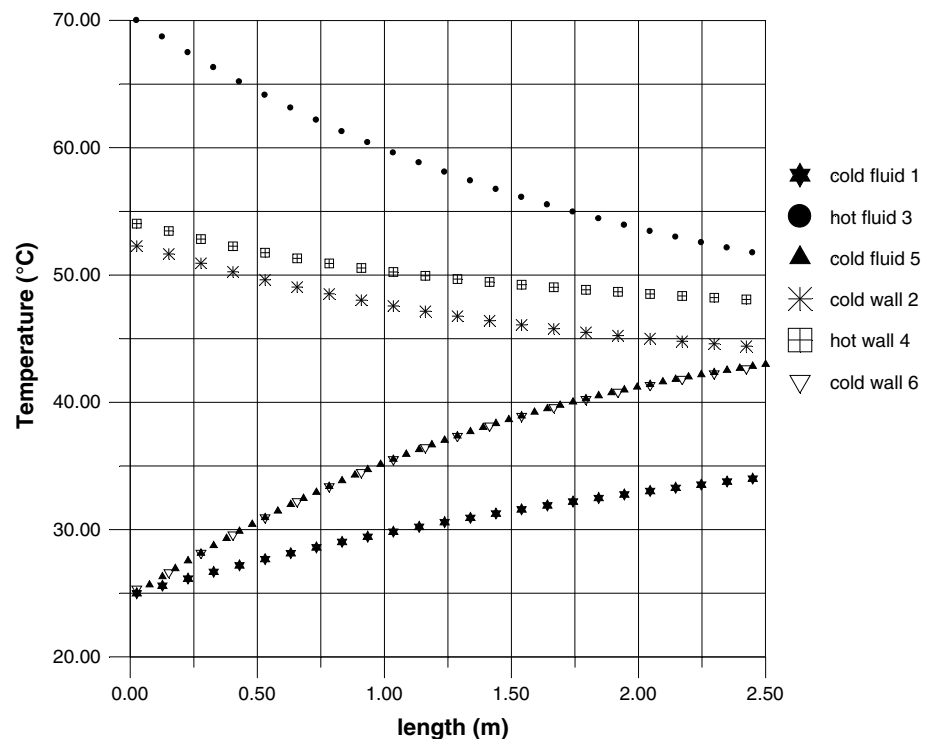
5 Conclusion

A numerical analysis is performed by using the method of finite differences to describe the unsteady state thermal behavior of a triple concentric-tube heat exchanger. The numerical results are validated in the steady state.

The results are presented as variation of temperatures of the three fluids and three walls with time along the heat exchanger.

The response of heat exchanger in parallel flow configuration is faster because the time lag is smaller; its performances are always lower than those of a counterflow heat

Fig. 13 Temperature profiles of the three fluids and three walls in steady state (parallel flow arrangement)



exchanger. The three fluids have a time lag for parallel flow, this time lag is more important for both cold fluids, what is not the case for the counterflow, because the only fluid that have a time lag is the hot fluid.

The heat transfer coefficients vary with time in addition to the temperature and the heat exchanges are lower in unsteady state than the steady state case.

References

- Morley TB (1933) Exchange of heat between three fluids. *Engineer* 155:134
- Rabinovich GD (1961) Steady state heat transfer among three streams in a parallel flow recuperator. *Inzh.-Fiz. Zh4* 11:37–43 (in Russian)
- Wolf J (1964) General solution of the equations of parallel flow multichannel heat exchangers. *Int J Heat Mass Transf* 7(8):901–919
- Aldous DD (1966) An analytical method for the design of a three-channel heat exchanger for cryogenic applications. M.S. thesis, Louisiana Polytechnic Institute, Ruston, Louisiana
- Zuritz CA (1990) On the design of triple concentric-tube heat exchangers. *J Food Process Eng* 12(2):113–130
- Ūnal A (1998) Theoretical analysis of triple concentric-tube heat exchangers Part 1: mathematical modelling. *Int Commun Heat Mass Transf* 25(7):949–958
- Ūnal A (2001) Theoretical analysis of triple concentric-tube heat exchangers Part 2: case studies. *Int Commun Heat Mass Transf* 28(2):243–256
- Sahoo PK, Ansari MIA, Datta AK (2003) A computer based iterative solution for accurate estimation of heat transfer coefficients in helical tube heat exchanger. *J Food Eng* 58:211–214
- Batmaz E, Sandeep KP (2005) Calculation of overall heat transfer coefficients in a triple tube heat exchangers. *Heat Mass Transf* 41:271–279
- Batmaz E, Sandeep KP (2008) Calculation of overall heat transfer coefficients and axial temperature distribution in a triple tube heat exchangers. *J Food Process Eng* 31:260–279
- Radulescu S, Negoita IL, Onutu I (2012) Heat transfer coefficient solver for a triple concentric-tube heat exchanger in transition regime. *Rev Chim (Buchar)* 8:820–824
- Quadir GA, Jarallah SS, Salman NJ, Badruddin IA (2013) Experimental investigation of the performance of a triple concentric pipe heat exchanger. *Int J Heat Mass Transf* 62:562–566
- Quadir GA, Badruddin IA, Salman NJ (2014) Numerical investigation of the performance of a triple concentric pipe heat exchanger. *Int J Heat Mass Transf* 75:165–172
- Pătrășcioiu C, Rădulescu S (2015) Prediction of the outlet temperatures in triple concentric-tube heat exchangers in laminar flow regime: case study. *Heat Mass Transf* 51:59–66
- Behera VM, Das DH, Nayak A (2014) Numerical analysis of triple tube heat exchanger using ANSYS. *Int J Sci Eng Res* 5(11):1226–1231
- Kac S, Yener Y (1987) Transient forced convection in ducts, *Handbook of single phase convective heat transfer*. Wiley, New York
- Valladares OG (2004) Numerical simulation of triple concentric pipe heat exchangers. *Int J Therm Sci* 43:979–991
- Nema PK, Datta AK (2005) A computer based solution to check the drop in milk outlet temperature due to fouling in a tubular heat exchanger. *J Food Eng* 71:133–142
- Bielski S, Malinowski L (2005) An analytical method for determining transient temperature field in a parallel-flow three-fluid heat exchanger. *Heat Mass Transf* 32:1034–1044
- Nema PK, Datta AK (2006) Improved milk fouling simulation in a helical triple tube heat exchanger. *Int J Heat Mass Transf* 49:3360–3370

21. Spalding DB (1972) A novel finite-difference formulation for differential expressions involving both first and second derivatives. *Int J Numer Methods Eng* 4:551–559
22. Nougier JP (1991) *Méthodes de calcul numérique*, 3rd edn. Masson, Paris
23. Sieder EN, Tate GE (1936) Heat transfer and pressure drop of liquids in tubes. *Ind Eng Chem* 28(12):1429–1435
24. El-Wakil N, Lachi M, Guellal M, Padet J (1995) Transient behaviour of shell and tube heat exchangers. *Eurotherm Seminar* 46, Pisa, Italy, pp 141–147
25. Guellal M, Abdesselam H (2009) Empirical correlation for the time lag of double pipe heat operating with variable flow rates. *Energy Convers Manag* 50:970–976